11264 *Biochemistry* **2009,** *48,* 11264–11272
DOI: 10.1021/bi900996q

BIOCHEMISTRY
including biophysical chemistry & molecular biology
Article

Fluorescence and UV Resonance Raman Study of Peptide−Vesicle Interactions of Human Cathelicidin LL-37 and Its F6W and F17W Mutants[†]

Jonathan E. Gable,[‡] Diana E. Schlamadinger,[‡] Anna L. Cogen,[§,∥] Richard L. Gallo,[§,⊥] and Judy E. Kim*[,‡]

[‡]*Department of Chemistry and Biochemistry and* [§]*Division of Dermatology and* [∥]*Department of Bioengineering, University of California at San Diego, La Jolla, California 92093, and* [⊥]*Veterans Affairs San Diego Healthcare System, San Diego, California 92161*

Received June 12, 2009; Revised Manuscript Received October 8, 2009

ABSTRACT: LL-37 is a broad-spectrum human antimicrobial peptide in the cathelicidin family. Potency assays in the form of minimal inhibitory concentration and vesicle leakage indicate that the single-tryptophan mutants, F6W and F17W, are as effective at killing bacteria and disrupting membranes as the native, tryptophan-free LL-37 peptide. Steady-state fluorescence and UV resonance Raman spectroscopy of F6W and F17W reveal molecular details of these tryptophan residues. The local environment polarity, hydrogen bond strength of the indole N−H moiety, and rotational freedom decrease for both F6W and F17W in the presence of carbonate ions relative to in pure distilled water; these results are consistent with burial of the hydrophobic region of α-helical LL-37 in oligomeric cores induced in the presence of carbonate ions. Differences in the spectroscopic properties of the carbonate-induced α-helical forms of F6W and F17W reflect the presence of a local lysine residue near F6W that makes the microenvironment of F6W more polar than that of F17W. In the presence of lipid vesicles, the mutants undergo additional loss of environment polarity, hydrogen bond strength, and rotational freedom. Quenching experiments utilizing brominated lipids reveal that the tryptophan residues in both mutants are essentially equidistant from the bilayer center and that bromines closer to the bilayer center, in the 9,10 positions, quench fluorescence more efficiently than those closer to the headgroups (6,7 positions). These results support carpeting or toroidal pore mechanisms of membrane disruption by LL-37 and demonstrate that the combination of tryptophan mutants and sensitive spectroscopic tools may provide important molecular clues about antimicrobial action.

Two major classes of antimicrobial peptides (AMPs)[1] have been identified in the human innate immune system, the cathelicidins and defensins (*1*). LL-37 is derived from the only human cathelicidin gene identified to date, hCAP18, and is expressed primarily in neutrophils and epithelial cells (*2*). Like the majority of antimicrobial peptides found in nature, LL-37 is cationic with an overall charge of +6. Its functional structure is an α-helix with a primary sequence of LLGDFFRKSKEKIGKEFKRIVQRIKDFLRNLVPRTES (*3*); a helical wheel is shown (Supporting Information Figure S1). LL-37 exhibits broad-spectrum antimicrobial activity, binds and neutralizes bacterial lipopolysaccharide, plays a role in wound healing, and is directly and indirectly chemotactic (*1*, *3*, *4*). The expression and activity of LL-37 have been implicated in a variety of medical conditions, including rosacea, atopic dermatitis, psoriasis, cystic fibrosis, and susceptibility to group A streptococci infection (*1*, *5*). The importance of this abundant human AMP in immunity and disease combined with the lack of detailed structural information on LL-37−membrane interactions motivates the current report.

General understanding of the membrane-disrupting activity of AMPs has improved in recent years, but specific molecular details remain unknown. In-depth studies of these ubiquitous peptides have largely been hindered by the inherent complexity of peptide−membrane systems as well as lack of practical tools for the study of AMPs at the molecular level. Here we employ the structurally sensitive technique of ultraviolet resonance Raman (UVRR) spectroscopy combined with a variety of fluorescence tools on LL-37 and two single-tryptophan mutants to elucidate a molecular picture of peptide−membrane interactions.

Tryptophan has been extensively utilized as a natural spectroscopic probe for studying membrane proteins and peptides, largely due to its intrinsic fluorescence and high propensity for the membrane−water interface (*6*, *7*). In addition to displaying environment- and structure-sensitive photophysics, tryptophan is ideal because it can be introduced into some classes of AMPs with minimal perturbation of the structure (*8*, *9*). The current study combines the well-characterized fluorescence and UVRR signals of tryptophan to reveal changes in local environment and structure (*10*). Comparison of these vibrational and fluorescence spectra of LL-37 in solution and bound to synthetic membranes provides valuable insight into the functional structures and

[†]J.E.G. is grateful for a UCSD Chancellor's Undergraduate Summer Research Scholarship, and D.E.S. acknowledges support from the UCSD MBTG NIH training grant (GM 08326). This work was partially supported by an NSF CAREER award to J.E.K.

*Corresponding author: e-mail, judyk@ucsd.edu; phone, 858-534-8080; fax, 858-534-7042.

[1]Abbreviations: AMP, antimicrobial peptide; POPG, 1-palmitoyl-2-oleoyl-*sn*-glycero-3-[phospho-*rac*-(1-glycerol)]; POPC, 1-palmitoyl-2-oleoyl-*sn*-glycero-3-phosphocholine; PSPC, 1-palmitoyl-2-stearoyl-*sn*-glycero-3-phosphocholine; Br(6,7)PC, 1-palmitoyl-2-stearoyl(6−7)dibromo-*sn*-glycero-3-phosphocholine; Br(9,10)PC, 1-palmitoyl-2-stearoyl(9−10)-dibromo-*sn*-glycero-3-phosphocholine; DI, deionized; ANTS, 8-aminonaphthalene-1,3,6-trisulfonate; DPX, *p*-xylenebis(pyridinium) bromide; MIC, minimal inhibitory concentration; CFU, colony-forming unit; CD, circular dichroism; UVRR, UV resonance Raman; TOE, tryptophan octyl ester; SUV, small unilamellar vesicle; FD, Fermi doublet; mCRAMP, mouse cathelin-related antimicrobial peptide; EDTA, ethylenediaminetetraacetic acid.

 Published on Web 11/06/2009

supports the carpeting and toroidal pore mechanisms of membrane disruption by this human cathelicidin.

MATERIALS AND METHODS

Chemicals. Wild-type LL-37 and mouse cathelicidin (mCRAMP) were obtained as previously described (*11*) as well as purchased with >95% purity from Anaspec (San Jose, CA). LL-37 mutants F6W and F17W were purchased with >95% purity from Genscript (Piscataway, NJ) and used without further purification. Anionic lipid 1-palmitoyl-2-oleoyl-*sn*-glycero-3-[phospho-*rac*-(1-glycerol)] (sodium salt, POPG), neutral lipids 1-palmitoyl-2-oleoyl-*sn*-glycero-3-phosphocholine (POPC) and 1-palmitoyl-2-stearoyl-*sn*-glycero-3-phosphocholine (PSPC), and brominated lipids 1-palmitoyl-2-stearoyl(6−7)dibromo-*sn*-glycero-3-phosphocholine (Br(6,7)PC) and 1-palmitoyl-2-stearoyl(9−10)dibromo-*sn*-glycero-3-phosphocholine (Br(9,10)PC) were purchased from Avanti Polar Lipids as chloroform solutions. Triton X-100 (Triton X) detergent was purchased from MP Biomedicals, Inc. L-Tryptophan, sodium bicarbonate, monobasic sodium phosphate, acrylamide, and HPLC-grade deionized (DI) water were purchased from Fisher Scientific and used as received. Tryptophan octyl ester (TOE) was obtained from Chem Impex International, and the concentration for UVRR and fluorescence experiments was 40 μM in sodium phosphate buffer, pH 7.4, and 15 μM in the presence of vesicles. The buffer used for all LL-37 experiments was 50 mM sodium bicarbonate and 1.1 mM sodium monobasic phosphate at pH = 7.4. Dye leakage assays were performed using the fluorophore 8-aminonaphthalene-1,3,6-trisulfonate (ANTS) and the quencher *p*-xylenebis-(pyridinium) bromide (DPX) from Invitrogen.

Vesicle Preparation. Chloroform−lipid solutions were combined to yield the indicated molar ratios. The resulting solution was dried under a stream of argon. Dried lipids were resuspended in the appropriate buffer using a bath sonicator. For dye-containing vesicles, the buffer also contained 50 mM ANTS and 50 mM DPX. Small unilamellar vesicles (SUVs) were made by sonication of the lipid solution with a Branson ultrasonicator microtip and filtered through a 0.45 μm filter to remove titanium dust and other particulates. Dye-containing vesicle solutions were passed through a gravity-driven desalting column (Bio-Rad 10-DG) to separate free dye from vesicles. Vesicle solutions were allowed to equilibrate for 1−4 h at 37 °C prior to use. The lipid concentration, based on dilution of the initial lipid solution and used in experiments, was 1 mg/mL. Vesicles were characterized to have diameters of less than 100 nm by dynamic light scattering measurements.

Circular Dichroism. Peptide was incubated for 1−4 h at 37 °C in vesicle solutions or at room temperature in DI water and buffer solution. Spectra were obtained using a 2 mm path length cuvette on a Cary 61 spectropolarimeter with a final peptide concentration of 40 μM. Data were acquired at a constant temperature of 23 °C with a step size of 1 nm and acquisition time of 5 s. Buffer-only and vesicle blank spectra were also acquired and subtracted from corresponding peptide spectra.

Fluorescence Spectroscopy. Spectra were obtained on a Jobin Yvon Horiba Fluorolog-3 Model FL3-11 spectrofluorometer. For tryptophan fluorescence measurements, including quenching experiments, vesicle-containing solutions were allowed to incubate with peptide for 65 ± 5 min at 37 °C. DI water and buffer solutions were equilibrated with peptide for 1−2 h at 30 °C. The excitation wavelength was 290 nm, and the entrance and exit bandpass were 2.6 or 2.0 and 6 nm, respectively. The error in peak position is ±1 nm. Fluorescence measurements were recorded at a constant temperature of 30 °C. Steady-state anisotropy measurements were made by introducing vertical (V) or horizontal (H) polarizers in the excitation and emission paths and collecting fluorescence. The resulting fluorescence intensities I_{VV}, I_{VH}, I_{HH}, and I_{HV}, where the first and second subscripts refer to excitation and emission polarizations, respectively, were used to calculate the anisotropy at 350 nm, r_{350}.

For leakage experiments, dye-containing vesicle solutions were allowed to incubate with peptide for 65 ± 5 min at 37 °C (*12*, *13*). The excitation wavelength was 386 nm, and the bandpass for entrance and exit slits was set to 5 nm. Triton X detergent was added to dye-containing vesicle solutions to determine the maximum fluorescence intensity corresponding to 100% dye leakage. Control experiments of dye-containing vesicle solutions in the absence of peptide were also performed to measure spontaneous leakage of dyes. Fluorescence measurements were recorded at a constant temperature of 30 °C.

UV Resonance Raman Spectroscopy. The UVRR setup has been described elsewhere (*14*). Vibrational spectra of the single tryptophan residue were obtained by setting the fundamental wavelength to 912 nm to generate a 228 nm excitation beam. A typical sample volume of 2 mL was flowed through a 100 μm i.d., 160 μm o.d. vertically mounted fused silica capillary at a rate of 0.16 mL/min to ensure fresh sample for each laser pulse. The UV power was 2−3 mW at the sample. The peptide concentration was 40 μM, and ten 1 min spectra were collected and summed for all peptide samples. TOE spectra were collected with 230 nm excitation, and data were acquired for 30−60 min. UVRR spectra of all appropriate blank solutions were also collected and subtracted from corresponding peptide spectra. Accuracy was determined using ethanol peaks and was found to be ±2 cm^{-1}. The bandpass was 11 cm^{-1}. The error for relative intensities is ~10%.

Minimal Inhibitory Concentration. The method to determine minimal inhibitory concentration (MIC) is a modification of a previously published protocol (*15*). Briefly, *Staphylococcus aureus* (*S. aureus*) 113 was grown to mid-log phase in media containing 20% tryptic soy broth, 1.1 mM dibasic sodium phosphate, and 50 mM sodium bicarbonate, pH 7.4. *S. aureus* at 10^5 CFU/mL was incubated with final concentrations of 0, 2, 4, 8, 16, 32, and 64 μM peptides LL-37, F6W, and F17W in the media. After 4 h of incubation at 37 °C, bacteria were plated on Todd Hewitt agar and enumerated for CFU. MIC measurements were performed a total of six times for each peptide.

RESULTS

Circular dichroism (CD) spectra of LL-37 and its mutants, F6W and F17W, in DI water, buffer, and anionic vesicles are shown in Figure 1. All peptides exhibit similar secondary structure in the tested conditions and are consistent with previous reports (*3*, *16*). Spectra characteristic of random coil were observed for peptide in DI water. In buffer and anionic vesicle solutions the peptides have α-helical secondary structure consistent with the CD minima at 208−210 and 222 nm as well as a maximum at 193−196 nm.

Fluorescence leakage assay results are presented in Figure 2 for LL-37, F6W, F17W, and the mouse cathelicidin mCRAMP at peptide concentrations up to ~40 μM. The comparison to mCRAMP was motivated by previous findings that LL-37 and

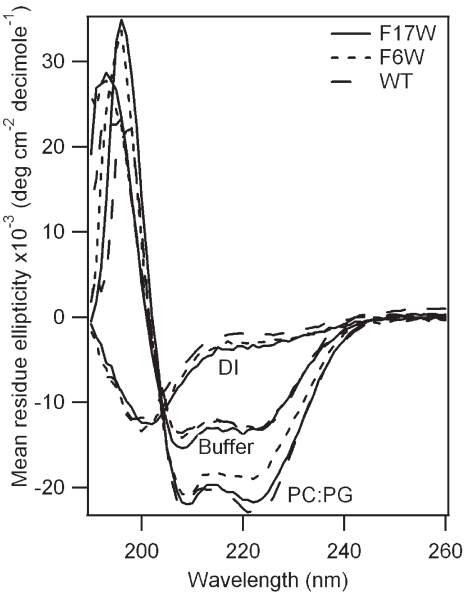

FIGURE 1: Circular dichroism spectra of F17W (solid), F6W (dotted), and wild-type (dashed) LL-37 in 2:1 POPC:POPG vesicles, buffer, and DI water.

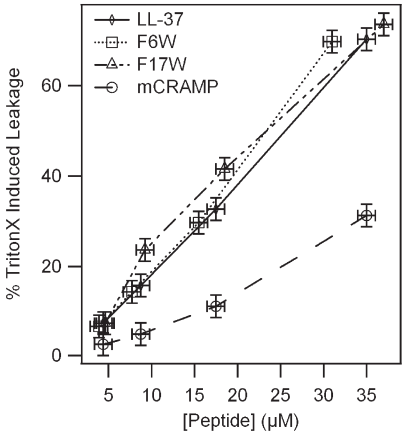

FIGURE 2: Fluorescence leakage assay results for native LL-37, F6W, F17W, and mouse cathelicidin mCRAMP. The ordinate indicates the fluorescence signal of the peptide relative to 100% leakage due to complete disruption of vesicles by Triton X detergent.

mCRAMP exhibit different potencies (*15*, *17*), and this variation in potency is supported by the leakage assay data. Within this concentration range there is no spectroscopic evidence of enhanced peptide−peptide interactions in the presence of vesicles (Supporting Information Figure S2). Peptide-induced leakage is reported relative to Triton X-induced leakage, which is 100%. Leakage depended linearly on peptide concentration for the range 5−40 μM. Scattering from vesicles was present at all concentrations after 1 h of incubation with peptide (data not shown). The MICs for LL-37 and both single-tryptophan mutants against *S. aureus* were 4 μM based on the following observation: in ~80% of the trials, the number of CFUs decreased over 80% in the presence of 4 μM peptide relative to 2 μM peptide, and in the presence of 8 μM peptide, 100% of the cells were killed for all trials. The observed MIC value of ~4 μM for LL-37 is consistent with prior reports (*15*).

Normalized steady-state tryptophan fluorescence spectra of 40 μM F6W and F17W in the presence of anionic vesicles, buffer, and DI water are shown in Figure 3. Fluorescence maxima

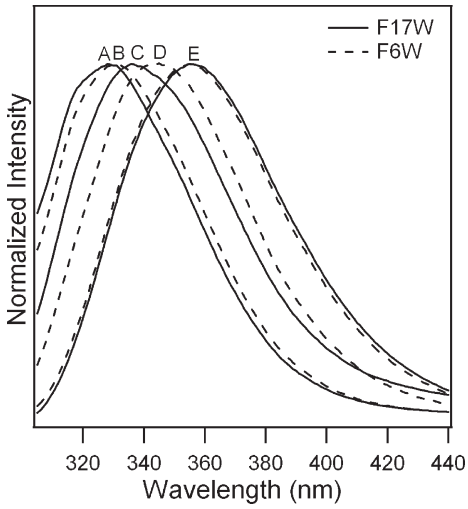

FIGURE 3: Steady-state tryptophan fluorescence spectra of single-tryptophan mutants F17W (solid) and F6W (short dash) in the presence of vesicles (A, B), carbonate buffer (C, D), and DI water (E). Spectra were normalized to a maximum emission intensity of unity; the normalization factor varied from 1.9×10^6 to 3.6×10^6 counts/s. All samples had a final peptide concentration of ~40 μM.

were most blue shifted in the presence of anionic vesicles with emission maxima at 330 and 328 nm for F6W and F17W, respectively. In buffer, the fluorescence maxima are 344 and 336 nm for F6W and F17W, respectively. Peptide in DI water yielded spectra with emission maxima values similar to that of 50 μM model compound L-tryptophan (358 nm); F6W and F17W in DI water exhibit maxima of 354 and 355 nm, respectively. A summary of fluorescence maxima is presented in Table 1.

Tryptophan fluorescence steady-state anisotropy values measured at 350 nm (r_{350}) are also summarized in Table 1. Model compound L-tryptophan yielded an anisotropy value of 0.02 ± 0.01 in DI water, in buffer, and in the presence of vesicles and a value of 0.05 ± 0.01 in 99% glycerol. In DI water, peptides exhibited r_{350} values of 0.04 ± 0.01 and 0.03 ± 0.01 for F6W and F17W, respectively. In buffer, r_{350} values of 0.06 ± 0.01 and 0.08 ± 0.01 were observed for F6W and F17W, respectively. Rotation was further hindered in the presence of vesicles, with anisotropy values of 0.10 ± 0.01 and 0.12 ± 0.01 for F6W and F17W, respectively.

Figures 4 and 5 present tryptophan fluorescence spectra in the presence of brominated lipids for peptide concentrations of 10, 20, and 40 μM. Bromines in the 9,10 positions quenched tryptophan fluorescence more efficiently than bromines in the 6,7 positions for both F6W and F17W over this concentration range. Although quenching varied with bromine position, all recorded fluorescence intensity values were within 62−76% of the fluorescence intensity in the absence of quenching. The relative fluorescence values, F/F_0, where F and F_0 are fluorescence intensities in the presence and absence of brominated lipids, respectively, are summarized in Table 2.

Excitation with 228 nm selectively enhances Raman scattering from tryptophan residues (*18*, *19*). Figure 6 and Supporting Information Figure S3 show UVRR spectra of F17W and F6W in anionic vesicles, buffer, and DI water. The labeled tryptophan peaks W3, W7, and W10 have been shown to be sensitive to local environment (*10*, *18*, *20*−*23*). The W10 doublet ratio, R_{W10}, is equal to $I_{\sim1240}/I_{\sim1250}$ and changes from 2.1 in DI water to 0.9 in anionic vesicles for F6W and from 1.8 (DI water) to 1.0 (anionic vesicles) for F17W. The Fermi doublet ratio, R_{FD}, is equal to

Table 1: Spectroscopic Values for L-Tryptophan, F6W, and F17W in DI Water, Buffer, and Vesicle: Emission Maximum (λ_{max}), UVRR Ratios R_{FD} and R_{W10}, and Anisotropy Value r_{350}

	DI water				buffer				vesicle			
sample	λ_{max}	R_{FD}	R_{W10}	r_{350}	λ_{max}	R_{FD}	R_{W10}	r_{350}	λ_{max}	R_{FD}	R_{W10}	r_{350}
L-Trp	358	1.0	2.5−3.5	0.02	358	1.0	2.5−3.5	0.02	358	1.1	2.5−3.5	0.02
F6W	354	1.2	2.1	0.04	344	1.7	1.3	0.06	330	2.1	0.9	0.10
F17W	355	1.4	1.8	0.03	336	2.0	1.1	0.08	328	2.3	1.0	0.12

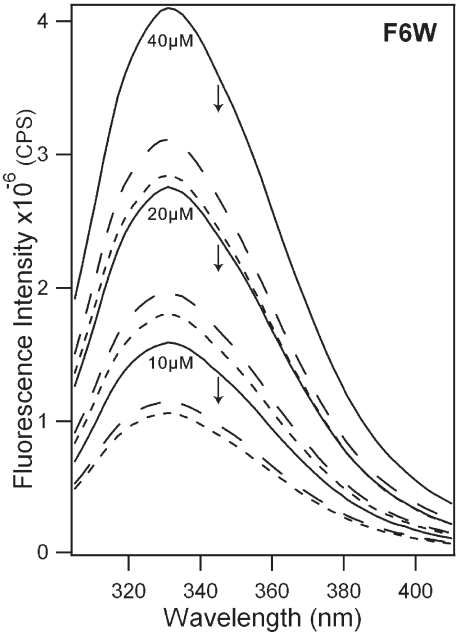

FIGURE 4: Fluorescence spectra of F6W in the presence of 1:1:1 POPC:POPG:PSPC (solid), 1:1:1 POPC:POPG:Br(6,7)PC (long dash), and 1:1:1 POPC:POPG:Br(9,10)PC (short dash) vesicles. Peptide concentrations are indicated. Downward arrows indicate decrease in fluorescence intensity in the presence of brominated lipid.

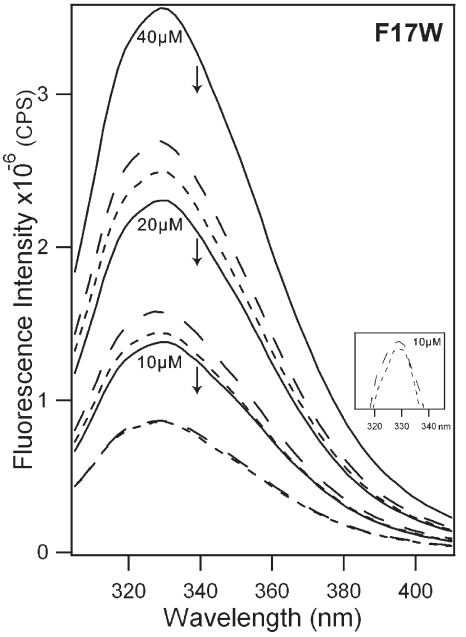

FIGURE 5: Fluorescence spectra of F17W in the presence of 1:1:1 POPC:POPG:PSPC (solid), 1:1:1 POPC:POPG:Br(6,7)PC (long dash), and 1:1:1 POPC:POPG:Br(9,10)PC (short dash) vesicles. Peptide concentrations are indicated. Downward arrows indicate decrease in fluorescence intensity in the presence of brominated lipid.

$I_{\sim1360}/I_{\sim1340}$ and shifts from 1.2 to 2.1 for F6W in DI water and anionic vesicles, respectively. For F17W, R_{FD} shifts from 1.4 to 2.3 in DI water and anionic vesicles, respectively. The W3 mode is sensitive to torsion angle $\chi^{2,1}$ and shows frequency variations in DI water, buffer, and anionic vesicle solutions. For F6W the frequencies correspond to $\chi^{2,1}$ angles of 95° in DI water (W3 = 1551 cm^{-1}), 102° in carbonate buffer (W3 = 1554 cm^{-1}), and 100° in vesicle solutions (W3 = 1553 cm^{-1}). W3 peak positions for F17W correspond to $\chi^{2,1}$ values in DI water, carbonate buffer, and vesicles of 98° (W3 = 1552 cm^{-1}), 108° (W3 = 1556 cm^{-1}), and 104°(W3 = 1554 cm^{-1}), respectively (*20*−*23*). UVRR R_{FD} and R_{W10} data are summarized in Table 1.

Table 2: Relative Fluorescence Intensity (F/F_0) for 10, 20, and 40 μM F6W and F17W in the Presence of Brominated Lipids

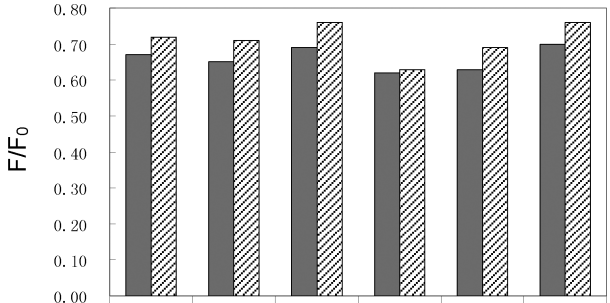

	10μM F6W	20μM F6W	40μM F6W	10μM F17W	20μM F17W	40μM F17W
9,10 Br-PC	0.67	0.65	0.69	0.62	0.63	0.70
6,7 Br-PC	0.72	0.71	0.76	0.63	0.69	0.76

DISCUSSION

Molecular level structure−function relationships are complex and not fully understood for amphipathic α-helical AMPs (*24*). This study aims to elucidate mechanistic details of cathelicidin LL-37, a major peptide of the human innate immune system that is primarily expressed by epithelial cells and neutrophils (*2*). Here, we probe the mechanisms by which LL-37 acts on synthetic vesicles by utilizing single-point mutations in which a native phenylalanine residue was converted to a tryptophan residue in position 6 or 17 to yield two mutant LL-37 peptides, F6W and F17W. The current study complements and builds upon the only other LL-37 tryptophan mutant, F27W (*8*), studied via spectroscopy; our focus on the F6W and F17W mutants permits analysis of the N-terminus and central portion of the peptide and thereby helps to provide a comprehensive molecular picture of peptide−membrane interactions. In addition to gaining insight

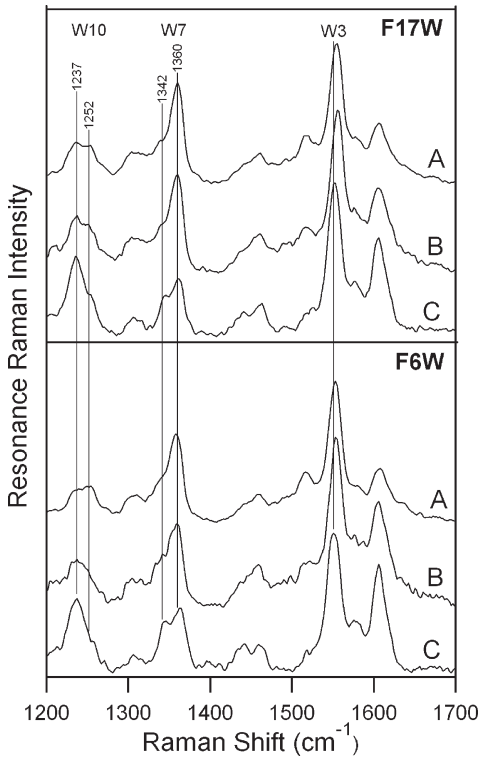

FIGURE 6: UVRR spectra of F17W (top) and F6W (bottom) in 2:1 POPC:POPG vesicles (A), buffer (B), and DI water (C). Normal modes W10, W7 (Fermi doublet), and W3 are indicated. Spectra are normalized to the W18 peak at ~770 cm^{-1} and offset for clarity.

into LL-37, the current study seeks, for the first time, to combine the structurally sensitive technique of UVRR with a wide variety of fluorescence techniques as general tools for the study of AMPs.

Potency of LL-37 Mutants. A single point mutation in position 6 or 17 from phenylalanine to tryptophan did not affect the antimicrobial activity of LL-37 against *S. aureus* nor its ability to cause leakage of 2:1 POPC:POPG vesicles. Furthermore, secondary structure differences were negligible in all tested conditions. Similar results have been reported previously; mutation from phenylalanine to tryptophan in position 27 of LL-37 was shown to have negligible effect on antimicrobial activity against *B. subtilis* and *S. aureus* as well as negligible effect on secondary structure (*8*). The lack of observable change in peptide potency upon incorporation of a tryptophan residue may be counterintuitive since thermodynamic studies have indicated that tryptophan partitions into the bilayer interface more readily than phenylalanine (*7*). In addition to having the largest thermodynamic driving force for insertion into bilayer interfaces, tryptophan plays a unique and essential role in transmembrane and membrane-associated proteins and peptides due to its dipole, aromaticity, nonpolar surface area, and ability to form a hydrogen bond (*25*−*28*).

While tryptophan is an important residue in membrane-associated proteins, the LL-37 results described here are not without precedent. Single-tryptophan mutants of magainin-2 F5W and F16W were equipotent against *Escherichia coli* and in causing leakage from anionic large unilamellar vesicles relative to wild type (*9*, *29*). The F12W mutation in magainin-2 appeared to augment antibacterial and hemolytic activities (*30*); however, there is some uncertainty in this interpretation (*9*, *31*). Tryptophan to phenylalanine mutations of all five tryptophan residues (38% of the peptide by residue count) of indolicidin (*32*) and the single-tryptophan residue of cecropin (*33*) had negligible effect on antimicrobial activity but lessened or eliminated hemolytic activity. While the replacement of phenylalanine with tryptophan has varying effects on peptide potency, omission of the single tryptophan residue in cecropin (*33*) and melittin (*34*) greatly reduced both hemolytic and antimicrobial activities, suggesting that aromatic residues as a general class are critical. Our observation that the phenylalanine-to-tryptophan mutation in LL-37 had negligible structural and potency effects relative to wild type is consistent with these and other reports and supports the use of these mutations to elucidate LL-37 action.

LL-37 Structures and Environments in Solution. The solution structures and local environments of F6W and F17W in DI water and buffer were observed with CD, UVRR, and fluorescence techniques. In DI water, wild type, F6W, and F17W CD spectra indicate a random coil secondary structure, consistent with previous findings (*16*); UVRR and tryptophan fluorescence spectra indicate tryptophan−solvent interactions similar to those of the solvated model compound L-tryptophan. The Fermi doublet ratio, R_{FD}, has previously been shown to be an indicator of the hydrophobicity of the local tryptophan environment (*10*−*12*), and we have recently demonstrated that the W10 ratio, R_{W10}, is an indicator of the strength of hydrogen bonding of the tryptophan indole N−H moiety. Specifically, R_{W10} increases with enhanced hydrogen bonding in both hydrophilic and hydrophobic environments (see Supporting Information Figure S4). R_{FD} values for both peptides in DI water indicate relatively hydrophilic environments; however, values in the 1.2−1.4 range suggest some solvent exclusion relative to free L-tryptophan. This difference in environment is consistent with the blue-shifted (~3 nm) fluorescence maxima of peptide relative to L-tryptophan in DI water. R_{W10} values for the mutants suggest that tryptophan is strongly hydrogen bonded, presumably to solvent. Steady-state fluorescence anisotropy values show that tryptophan residues of LL-37 in DI water are relatively unhindered. In the concentration range of 4−40 μM, there is no indication of peptide aggregation in DI water. From these data we conclude that majority populations of both mutants in DI water lack well-defined secondary structure and are solvated by water.

The introduction of carbonate-containing buffer leads to the formation of α-helical secondary structure as determined by circular dichroism. Some, albeit less, α-helical structure was observed in 5 mM HEPES and 0.1 mM EDTA, pH 7.0, buffer for F27W (*8*). The formation of secondary structure in buffer is consistent with previous results for native LL-37, which suggested the formation of oligomers in the presence of some salts, including sodium bicarbonate (*16*). In the current experiments, sodium bicarbonate buffer was chosen because of its biological relevance in the context of AMP-expressing tissues (*35*, *36*) as well as studies that suggested that carbonate enhances susceptibility of bacteria to LL-37 (*15*). This increase in susceptibility has largely been attributed to carbonate's direct effect on the bacterial cell wall and membrane composition as well as alterations in gene expression, as opposed to a direct effect on LL-37 (*15*). However, since the disruptive activity of LL-37 on membranes is concomitant with the formation of α-helical structure, we were motivated to compare the α-helical structure induced via salt effects and interpeptide interactions with the membrane-bound, functional structure (*16*, *37*, *38*).

Upon formation of α-helical structure in the presence of carbonate ions, the tryptophan local environment of F6W and

F17W became more hydrophobic, and the extent of hydrogen bonding was reduced relative to the random coil conformation in DI water. This interpretation is based on increases in R_{FD} and decreases in R_{W10}, respectively. Fluorescence maxima in buffer were blue shifted relative to in DI water and remained constant from 0.5 to 40 μM (data not shown), indicating that the oligomeric state (*16*) is unchanged in the presence of carbonate in this concentration range. The anisotropy values are consistent with these UVRR and fluorescence results and suggest a decrease in tryptophan mobility upon burial in the hydrophobic core. The lower anisotropy value for F6W compared to F17W is consistent with 2D (*39*) and 3D (*40*) NMR structural data that showed that F6 of native LL-37 is considerably more mobile than F17. Collectively, these results support the picture, as has been suggested (*16*, *41*), that self-association of LL-37 may be driven by sequestration of the hydrophobic face of the peptide; this enhanced hydrophobicity is apparent in the current fluorescence and UVRR results of the tryptophan residues.

There are significant differences in the local tryptophan environments of F6W and F17W in buffer. The tryptophan of F17W experiences a more hydrophobic environment than does F6W based on both tryptophan fluorescence emission maxima and UVRR R_{FD} values, while the hydrogen-bonding indicator R_{W10} is equivalent for both peptides. In order to understand this difference in local environment, a recently published NMR structure (*40*) was modified to create models of F6W and F17W. The necessary single point mutation was added, and a sterically allowed rotamer consistent with $\chi^{2,1}$ values based on UVRR W3 frequencies was generated using Swiss-PDB Viewer DeepView (*9*, *14*, *32*). These models (Figure 7) illustrate that the tryptophan residue of F6W is in close proximity to Lys10 while the tryptophan residue of F17W is isolated from hydrophilic residues. Tryptophan location relative to charged residues within membrane-associated peptides has previously been shown to influence fluorescence emission maxima (*42*). The presence of Lys10 likely creates a more polar environment near W6 by direct and indirect effects. The center of the tryptophan residue (midpoint of the $C^{\delta2}-C^{\varepsilon2}$ bond) in our F6W model is approximately 7−8 Å away from the center of Phe5, suggesting only weak $\pi-\pi$ interaction (*43*, *44*). While these effects of tryptophan intramolecular localization and solvent accessibility contribute to the difference in local hydrophobicity, as reflected by R_{FD} and emission maxima values, this difference may also reflect inter-peptide interactions of the LL-37 multimer.

LL-37 Structure and Environment in Vesicles. In the presence of anionic vesicles, the peptides F6W, F17W, and native LL-37 exhibit strong α-helical content, consistent with previous studies of native LL-37 and mutant F27W (*4*, *15*, *35*, *36*). Fluorescence emission maxima are significantly blue shifted, anisotropy values indicate enhanced hindrance, R_{FD} values suggest hydrophobic environments, and R_{W10} values show further loss of hydrogen bonding compared to the α-helix in buffer. In combination with leakage assay data, these spectroscopic observations support strong peptide−vesicle interactions.

Analogous to peptide in carbonate buffer, the emission maximum for F17W is more blue shifted than that of F6W; however, the difference in emission maxima of ~180 cm^{-1} for these peptides in vesicle (330 vs 328 nm) is much smaller than the difference of ~690 cm^{-1} in buffer (344 vs 336 nm). Since the absorption maximum of tryptophan varies ~2−3 nm in membrane proteins, the fluorescence emission maxima roughly reflect the Stokes shift and can be compared across peptides.

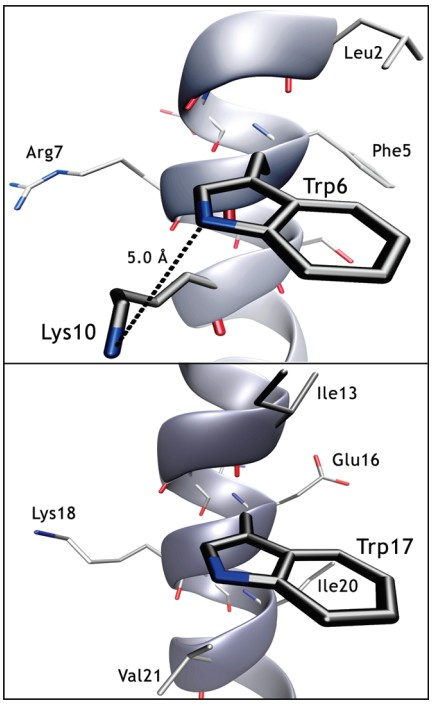

FIGURE 7: Model of the tryptophan residue of F6W (top) and F17W (bottom).

The difference in Stokes shift for a given condition represents an amalgamation of structural and environmental differences between peptide in buffer and bound to vesicle. In the presence of vesicles there is no change in emission maximum with peptide concentrations from 4 to 40 μM (Supporting Information Figure S2), consistent with a previous report that suggested a majority of vesicle-bound monomer population (*45*). Although these results show no indication of static multimer formation in the presence of anionic vesicles, these data do not exclude these conformations nor the possibility of transient multimeric pores proposed in other studies (*31*, *41*). Finally, the data presented here provide no evidence for amyloid-like fibril formation as has been reported for the LL-37 F27W mutant (*8*); this difference may be attributable to variations in vesicle and buffer composition as well as temperature and incubation time.

Comparison of UVRR spectra of LL-37 mutants to model tryptophan compounds that are known to reside at the bilayer−water interface indicates that the tryptophan residue in F6W and F17W likely does not interact closely with lipid headgroups. Tryptophan octyl ester (TOE) has previously been used as a model compound to study the properties of tryptophan localized in the interfacial region of phospholipid bilayers (*46*, *47*). We have measured the UVRR spectra of TOE (Supporting Information Figure S5). In 20 mM potassium phosphate buffer (pH 7.4), TOE exhibits a fluorescence emission maximum of 359 nm with R_{FD} and R_{W10} values of 1.1 and 2.4−2.8, respectively. TOE bound to POPC vesicles exhibits a fluorescence emission maximum of 343 nm with R_{FD} and R_{W10} values of 1.4 and 2.4−2.8, respectively. It appears that TOE in the POPC vesicle has greater hydrogen-bonding character than F6W or F17W in the presence of vesicles based on the R_{W10} values. This finding confirms that TOE is localized at the water−bilayer interface and is thus partially solvent-exposed, while the tryptophan residues of F17W and F6W are shielded from solvent due to penetration into the bilayer and/or to the presence of neighboring hydrophobic residues. The TOE spectrum also shows

evidence of cation−π interactions, with presumably the choline headgroup, based on alterations in the W18 and W16 peaks (*48*−*50*). Analogous analysis of the F6W and F17W UVRR spectra also suggests the presence of cation−π interactions, especially for F6W; the decrease in intensity of the W16 peak relative to the W18 peak is significant (∼15% relative to in DI water). Lys10 is a likely candidate for intramolecular cation−π interaction since it is in the $i + 4$ position relative to Trp6 (*51*). However, we do not eliminate the possibility of intermolecular cation−π interactions. Finally, comparison of the W3 peak widths of TOE and LL-37 reveals that the structural distribution of TOE is highly heterogeneous when bound to vesicles whereas the LL-37 distribution is less heterogeneous.

In order to better understand the position and orientation of LL-37 relative to the bilayer, brominated lipid quenching experiments were performed with both mutant peptides. Bromine pairs at varying positions along the lipid tail have previously been shown to cause distance-dependent tryptophan fluorescence quenching when tryptophan is inserted in the bilayer (*52*, *53*). Brominated lipids Br(6,7)-PC and Br(9,10)-PC were utilized. For both peptides, Br(9,10)-PC quenched tryptophan fluorescence more efficiently than Br(6,7)-PC. These data were analyzed using the parallax method to determine the distance from the center of the bilayer to tryptophan (*54*). The distance between the two bromine pairs, L_{21}, and distance from the center of the bilayer to the shallow quencher, L_{c1}, were taken to be 3 and 11 Å, respectively, based on X-ray diffraction data (*55*). Given these parameters, the average distance from the bilayer center to tryptophan, z_{cF}, for both F6W and F17W was ∼9 Å. This distance corresponds to a depth in the hydrophobic core of ∼6 Å. Given the uncertainty in the lipid bilayer dimensions and the assumptions and sensitivity of the parallax method, the accuracy of this measured depth is difficult to quantify. Regardless of this uncertainty the data support a picture in which the tryptophan of both F6W and F17W lies in the same plane. This finding is supported by Stern−Volmer plots for the peptides; acrylamide quenching data indicate that F6W and F17W have similar solvent accessibility (Supporting Information Figure S6). Similar data were reported for F27W which was found to have a z_{cF} value of 10 Å (*8*). Collectively, the quenching data for F6W, F17W, and F27W confirm that LL-37 is oriented parallel to the bilayer surface as was previously reported (*45*, *56*). These data are also in agreement with NMR studies which place the bottom of the amphiphilic helix of native LL-37 between C8 and C9 of the lipid acyl chain at a depth of 5−6 Å into the hydrophobic core (*41*).

Implications for LL-37 Mechanisms of Membrane Disruption. Four primary mechanisms of membrane disruption have been proposed for antimicrobial peptide activity: the barrel stave, toroidal pore, detergent, and carpeting models (*57*). More recently "peptide-induced demixing" has been proposed as a mechanism for activity. In this model, lipid−peptide domains form due to the electrostatic attraction between cationic AMPs and anionic lipid headgroups (*58*). The observation that vesicles remain intact based on fluorescence and dynamic light scattering measurements in the presence of LL-37 eliminates a detergent-like mechanism for complete dissolution of the vesicle in the 4−40 μM concentration range. The finding that tryptophan residues of F6W and F17W are at equivalent depths in the bilayer and experience similar environments consequently rules out the membrane-spanning orientation necessary for barrel stave formation. Instead, our data are consistent with carpeting, demixing, and toroidal pore mechanisms and, therefore, support prior work on LL-37 (*41*, *45*, *56*, *58*). This convergence of hypotheses based on a diverse set of experiments strengthens this model of AMP action for this ubiquitous α-helical peptide. In these scenarios, the lack of change in tryptophan emission maxima in the presence of vesicles as a function of peptide concentration suggests that the monomeric or multimeric state of the functional peptide is unaltered over the studied concentration range. It is likely that a combination of mechanisms is involved in membrane disruption. For example, monomeric LL-37 may first carpet the membrane, followed by lipid demixing; this demixing may disrupt the lipid bilayer and cause defects that allow leakage of intravesicular molecules (*56*).

Conclusion and Outlook. A growing body of evidence suggests that for many AMPs, in particular the α-helical and small unstructured peptides, conversion of phenylalanine to tryptophan and vice versa does not affect antimicrobial activity against Gram-negative and Gram-positive bacteria but, instead, significantly alters hemolytic activity (*8*, *9*, *30*, *32*, *33*). This finding is crucial for the design of peptides as novel antibiotic agents as well as for the design of spectroscopic experiments to probe mechanisms of AMP action. The abundance of aromatic amino acids makes UVRR a promising technique for gaining molecular level understanding of AMP activity; the experimental findings reported here may allow for site-specific spectroscopic studies of the 100+ helical and 700+ nonhelical tryptophan- or phenylalanine-containing peptides currently found in the antimicrobial database (*59*). A key advantage to UVRR is that it not only elucidates the structure and environment of aromatic residues, but this technique may be applied to reveal local microenvironment, including hydrogen-bonding states, of other residues including proline, histidine, cystine, cysteine, and methionine, as well as backbone structure (*21*−*23*). Furthermore, UVRR measurements can be made with very high time resolution, which allows for observation of membrane binding and secondary structure formation events in real time. UVRR and other inherently structure-sensitive tools will contribute to a fundamental understanding of the molecular interactions that govern antimicrobial activity and, hence, impact AMP engineering that may help to deter the growing number of antibiotic-resistant pathogens.

ACKNOWLEDGMENT

We thank Dr. Kenshi Yamasaki for insightful discussions, Professor Uli Müller for use of a vacuum concentrator, Professor Douglas Magde for use of dynamic light scattering instrumentation, and Dina Kats for assistance with acrylamide quenching experiments.

SUPPORTING INFORMATION AVAILABLE

Helical wheel, tryptophan fluorescence spectra for different peptide concentrations, full UVRR spectra of peptides, UVRR W10 region of the model compound in solvent mixtures, UVRR spectra of TOE, and Stern−Volmer plots. This material is available free of charge via the Internet at http://pubs.acs.org.

REFERENCES

1. Lai, Y., and Gallo, R. L. (2009) AMPed up on immunity: How antimicrobial peptides have multiple roles in immune defense. *Trends Immunol. 30*, 131–141.
2. Bals, R., Wang, X., Zasloff, M., and Wilson, J. M. (1998) The peptide antibiotic LL-37/hCAP-18 is expressed in epithelia of the human lung

where it has broad antimicrobial activity at the airway surface. *Proc. Natl. Acad. Sci. U.S.A. 95*, 9541–9546.
3. Turner, J., Cho, Y., Dinh, N.-N., Waring, A. J., and Lehrer, R. I. (1998) Activities of LL-37, a cathelin-associated antimicrobial peptide of human neutrophils. *Antimicrob. Agents Chemother. 42*, 2206–2214.
4. Carretero, M., Escámez, M. J., García, M., Duarte, B., Holguín, A., Retamosa, L., Jorcano, J. L., Río, M. D., and Larcher, F. (2008) *In vitro* and *in vivo* wound healing-promoting activities of human cathelicidin LL-37. *J. Invest. Dermatol. 128*, 223–236.
5. Gryllos, I., Tran-Winkler, H. J., Cheng, M.-F., Chung, H.III, R. B., Lu, W., Lehrer, R. I., and Wessels, M. R. (2008) Induction of group A *Streptococcus* virulence by a human antimicrobial peptide. *Proc. Natl. Acad. Sci. U.S.A. 105*, 16755–16760.
6. Clayton, A. H. A., and Sawyer, W. H. (2002) Site-specific tryptophan fluorescence spectroscopy as a probe of membrane peptide structure and dynamics. *Eur. Biophys. J. 31*, 9–13.
7. Wimley, W. C., and White, S. H. (1996) Experimentally determined hydrophobicity scale for proteins at membrane interfaces. *Nat. Struct. Biol. 3*, 842–848.
8. Sood, R., Domanov, Y., Pietiäinen, M., Kontinen, V. P., and Kinnunen, P. K. J. (2008) Binding of LL-37 to model biomembranes: Insight into target *vs* host cell recognition. *Biochim. Biophys. Acta 1778*, 983–996.
9. Matsuzaki, K., Murase, O., Tokuda, H., Funakoshi, S., Fujii, N., and Miyajima, K. (1994) Orientational and aggregational states of magainin 2 in phospholipid bilayers. *Biochemistry 33*, 3342–3349.
10. Takeuchi, H. (2003) Raman structural markers of tryptophan and histidine side chains in proteins. *Biopolymers 72*, 305–317.
11. Braff, M. H., Hawkins, M. I. A., Nardo, A. D., Lopez-Garcia, B., Howell, M. D., Wong, C., Lin, K., Streib, J. E., Dorschner, R., Leung, D. Y. M., and Gallo, R. L. (2005) Structure-function relationships among human cathelicidin peptides: Dissociation of antimicrobial properties from host immunostimulatory activities. *J. Immunol. 174*, 4271–4278.
12. Ellens, H., Bentz, J., and Szoka, F. S. (1984) pH-Induced destabilization of phosphatidylethanolamine-containing liposomes: Role of bilayer contact. *Biochemistry 23*, 1532–1538.
13. Wimley, W. C., Selsted, M. E., and White, S. H. (1994) Interactions between human defensins and lipid bilayers: Evidence for formation of multimeric pores. *Protein Sci. 3*, 1362–1373.
14. Sanchez, K. M., Neary, T. J., and Kim, J. E. (2008) Ultraviolet resonance Raman spectroscopy of folded and unfolded states of an integral membrane protein. *J. Phys. Chem. B 112*, 9507–9511.
15. Dorschner, R. A., Lopez-Garcia, B., Peschel, A., Kraus, D., Morikawa, K., Nizet, V., and Gallo, R. L. (2006) The mammalian ionic environment dictates microbial susceptibility to antimicrobial defense peptides. *FASEB J. 20*, 35–42.
16. Johansson, J., Gudmundsson, G. H., Rottenberg, M. E., Berndt, J. D., and Agerberth, B. (1998) Conformation-dependent antibacterial activity of the naturally occurring human peptide LL-37. *J. Biol. Chem. 273*, 3718–3724.
17. Gallo, R. L., Kim, K. J., Bernfield, M., Kozak, C. A., Zanetti, M., Merluzzi, L., and Gennaro, R. (1997) Identification of CRAMP, a cathelin-related antimicrobial peptide expressed in the embryonic and adult mouse. *J. Biol. Chem. 272*, 13088–13093.
18. Asher, S. A., Ludwig, M., and Johnson, C. R. (1986) UV resonance Raman excitation profiles of the aromatic amino acids. *J. Am. Chem. Soc. 108*, 3186–3197.
19. Rava, R. P., and Spiro, T. G. (1985) Resonance enhancement in the ultraviolet Raman spectra of aromatic amino acids. *J. Phys. Chem. 89*, 1856–1861.
20. Juszczak, L. J., and Desamero, R. Z. B. (2009) Extension of the tryptophan χ2,1 dihedral angle-W3 band frequency relationship to a full rotation: Correlations and caveats. *Biochemistry 48*, 2777–2787.
21. Austin, J. C., Jordan, T., and Spiro, T. G. (1993) Ultraviolet resonance Raman studies of proteins and related model compounds, in Biomolecular Spectroscopy (Advances in Spectroscopy), Part A (Clark, R. J. H., and Hester, R. E., Eds.) Wiley, New York.
22. Harada, I., and Takeuchi, H. (1986) Raman and ultraviolet resonance Raman spectra of proteins and related compounds, in Spectroscopy of Biological Systems (Clark, R. J. H., and Hester, R. E., Eds.) Wiley, Chichester.
23. Asher, S. A. (1988) UV resonance Raman studies of molecular structure and dynamics applications in physical and biophysical chemistry. *Annu. Rev. Phys. Chem. 39*, 537–588.
24. Tossi, A., Sandri, L., and Giangaspero, A. (2000) Amphipathic, α-helical antimicrobial peptides. *Biopolymers 55*, 4–30.
25. Yau, W.-M., Wimley, W. C., Gawrisch, K., and White, S. H. (1998) The preference of tryptophan for membrane interfaces. *Biochemistry 37*, 14713–14718.
26. Wolfenden, R. (2007) Experimental measures of amino acid hydrophobicity and the topology of transmembrane and globular proteins. *J. Gen. Physiol. 129*, 357–362.
27. Schiffer, M., Chang, C.-H., and Stevens, F. J. (1992) The function of tryptophan residues in membrane proteins. *Protein Eng. 5*, 213–214.
28. Chan, D. I., Prenner, E. J., and Vogel, H. J. (2006) Tryptophan- and arginine-rich antimicrobial peptides: Structures and mechanisms of action. *Biochim. Biophys. Acta 1758*, 1184–1202.
29. Matsuzaki, K., Mitani, Y., Akada, K.-y., Murase, O., Yoneyama, S., Zasloff, M., and Miyajima, K. (1998) Mechanism of synergism between antimicrobial peptides magainin 2 and PGLa. *Biochemistry 37*, 15144–15153.
30. Matsuzaki, K., Sugishita, K.-i., Harada, M., Fujii, N., and Miyajima, K. (1997) Interactions of an antimicrobial peptide, magainin 2, with outer and inner membranes of Gram-negative bacteria. *Biochim. Biophys. Acta 1327*, 119–130.
31. Matsuzaki, K., Murase, O., Fuji, N., and Miyajima, K. (1996) An antimicrobial peptide, magainin 2, induced rapid flip-flop of phospholipids coupled with pore fromation and peptide translocation. *Biochemistry 35*, 11361–11368.
32. Subbalakshmi, C., Krishnakumari, V., Nagaraj, R., and Sitaram, N. (1996) Requirements for antibacterial and hemolytic activities in the bovine neutrophil derived 13-residue peptide indolicidin. *FEBS Lett. 395*, 48–52.
33. Andreu, D., and Merrifield, R. B. (1985) N-terminal analogues of cecropin A: Synthesis, antibacterial activity, and conformational properties. *Biochemistry 24*, 1683–1688.
34. Blondelle, S. E., and Houghten, R. A. (1991) Hemolytic and antimicrobial activities of the twenty-four individual omission analogues of melittin. *Biochemistry 30*, 4671–4678.
35. McKay, W., Morris, R., and Mushlin, P. (1987) Sodium bicarbonate attenuates pain on skin infiltration with lidocaine, with or without epinephrine. *Anesth. Analg. 66*, 572–574.
36. Turnberg, L. A., Fordtran, J. S., Carter, N. W., Floyd, C., and Rector, J. (1970) Mechanism of bicarbonate absorption and its relationship to sodium transport in the human jejunum. *J. Clin. Invest. 49*, 548–556.
37. Zhang, Y., and Cremer, P. S. (2006) Interactions between macromolecules and ions: The Hofmeister series. *Curr. Opin. Chem. Biol. 10*, 658–663.
38. Cacace, M. G., Landau, E. M., and Ramsden, J. J. (1997) The Hofmeister series: Salt and solvent effects on interfacial phenomena. *Q. Rev. Biophys. 30*, 241–277.
39. Porcelli, F., Verardi, R., Shi, L., Henzler-Wildman, K. A., and Ramamoorthy, A. (2008) NMR structure of cathelicidin-derived human antimicrobial peptide LL-37 in dodecylphosphocholine micelles. *Biochemistry 47*, 5565–5572.
40. Wang, G. (2008) Structures of human host defense cathelicidin LL-37 and its smallest antimicrobial peptide KR-12 in lipid micelles. *J. Biol. Chem. 283*, 32637–32643.
41. Henzler-Wildman, K. A., Martinez, G. V., Brown, M. F., and Ramamoorthy, A. (2004) Perturbation of the hydrophobic core of lipid bilayers by the human antimicrobial peptide LL-37. *Biochemistry 43*, 8459–8469.
42. de Kroon, A. I. P. M., Soekarjo, M. W., de Gier, J., and de Kruijff, B. (1990) The role of charge and hydrophobicity in peptide-lipid interaction: A comparative study based on tryptophan fluorescence measurements combined with the use of aqueous and hydrophobic quenchers. *Biochemistry 29*, 8229–8240.
43. Samanta, U., Pal, D., and Chakrabarti, P. (1999) Packing of aromatic rings against tryptophan residues in proteins. *Acta Crystallogr., Sect. D: Biol. Crystallogr. 55*, 1421–1427.
44. Thomas, A., Meurisse, R., Charloteaux, B., and Brasseur, R. (2002) Aromatic side-chain interactions in proteins. I. Main structural features. *Proteins: Struct., Funct., Bioinf. 48*, 628–634.
45. Oren, Z., Lerman, J. C., Gudmundsson, G. H., Agerberth, B., and Shai, Y. (1999) Structure and organization of the human antimicrobial peptide LL-37 in phospholipid membranes: Relevance to the molecular basis for its non-cell-selective activity. *Biochem. J. 341*, 501–513.
46. Ladokhin, A. S., and Holloway, P. W. (1995) Fluorescence of membrane-bound tryptophan octyl ester: A model for studying intrinsic fluorescence of protein-membrane interactions. *Biophys. J. 69*, 506–517.
47. Chattopadhyay, A., Arora, A., and Kelkar, D. A. (2005) Dynamics of a membrane-bound tryptophan analog in environments of varying hydration: A fluorescence approach. *Eur. Biophys. J. 35*, 62–71.
48. Xue, Y., Davis, A. V., Balakrishnan, G., Stasser, J. P., Staehlin, B. M., Focia, P., Spiro, T. G., Penner-Hahn, J. E., and O'Halloran, T. V.

(2008) Cu(I) recognition via cation-π and methionine interactions in CusF. *Nat. Chem. Biol. 4*, 107–109.
49. Wen, Z. Q., George, J., and Thomas, J. (2000) Ultraviolet-resonance Raman spectroscopy of the filamentous virus Pf3: Interactions of trp38 specific to the assembled virion subunit. *Biochemistry 39*, 146–152.
50. Okada, A., Miura, T., and Takeuchi, H. (2001) Protonation of histidine and histidine-tryptophan interaction in the activation of the M2 ion channel from influenza A virus. *Biochemistry 40*, 6053–6060.
51. Shi, Z., Olson, C. A., and Kallenbach, N. R. (2002) Cation-π interaction in model α-helical peptides. *J. Am. Chem. Soc. 124*, 3284–3291.
52. Devaux, P. F., and Seigneuret, M. (1985) Specificity of lipid-protein interactions as determined by spectroscopic techniques. *Biochim. Biophys. Acta 822*, 63–125.
53. Bolen, E. J., and Holloway, P. W. (1990) Quenching of tryptophan fluorescence by brominated phospholipid. *Biochemistry 29*, 9638–9643.
54. Abrams, F. S., and London, E. (1992) Calibration of the parallax fluorescence quenching method for determination of membrane penetration depth: Refinement and comparison of quenching by spin-labeled and brominated lipids. *Biochemistry 31*, 5312–5322.
55. McIntosh, T. O., and Holloway, P. W. (1987) Determination of the depth of bromine atoms in bilayers formed from bromolipid probes. *Biochemistry 26*, 1783–1788.
56. Henzler-Wildman, K. A., Lee, D.-K., and Ramamoorthy, A. (2003) Mechanism of lipid bilayer disruption by the human antimicrobial peptide, LL-37. *Biochemistry 42*, 6545–6558.
57. Brogden, K. A. (2005) Antimicrobial peptides: zPore formers or metabolic inhibitors in bacteria? *Nat. Rev. Microbiol. 3*, 238–250.
58. Arouri, A., Dathe, M., and Blume, A. (2009) Peptide induced demixing in PG/PE lipid mixtures: A mechanism for the specificity of antimicrobial peptides towards bacterial membranes? *Biochim. Biophys. Acta 1788*, 650–659.
59. Wang, Z., and Wang, G. (2004) APD: The antimicrobial peptide database. *Nucleic Acids Res. 32*, D590–D592.